Directed assembly of acac-based complexes by deliberately fine-tuning electrostatic molecular-recognition events

*Boris-Marko Kukovec,[a] Magdalena Malik,[b] Ivan Kodrin,[a] Christer B. Aakeröy[c] and Marijana Đaković[a]**

[a] Department of Chemistry, Faculty of Science, University of Zagreb, Horvatovac 102a, HR-10000 Zagreb, Croatia

[b] Faculty of Chemistry, Wrocław University of Technology, Smoluchowskiego 23, 50-370 Wrocław, Poland

[c] Department of Chemistry, Kansas State University, Manhattan, KS, 66506, USA

Supplementary Information

Table of Contents

1. Single crystal X-ray crystallography

Table S1. Crystal data and details of the structure determination for **1a**−**4a**.

Compound	**1a**	**2a**	**3a**	**4a**
Formula	$C_{42}H_{34}CoN_4O_6$	$C_{44}H_{38}CoN_4O_6$	$C_{42}H_{34}CoN_4O_6$	$C_{44}H_{38}CoN_4O_6$
M_r	749.66	777.71	749.66	777.71
Colour and habit	orange, prism	orange, plate	orange, block	orange, block
Crystal system, space group	monoclinic, $C2/c$	monoclinic, $P2_1/c$	triclinic, P-1	triclinic, P-1
Crystal dimensions (mm^3)	0.34 × 0.23 × 0.18	0.33 × 0.29 × 0.07	0.92 × 0.73 × 0.36	0.41 × 0.30 × 0.22
a (Å)	16.9322(10)	18.7191(7)	8.6802(4)	8.1160(5)
b (Å)	11.1599(5)	10.3356(4)	9.5380(5)	10.6934(6)
c (Å)	20.1747(10)	20.7415(7)	23.3235(10)	11.9794(8)
α (˚)	90	90	79.455(4)	111.926(6)
β (˚)	106.529(6)	109.898(4)	85.277(4)	92.140(5)
γ (˚)	90	90	74.976(4)	99.865(5)
V ($Å^3$)	3654.7(3)	3773.4(2)	1832.25(15)	944.34(10)
Z	4	4	2	1
D_{calc} (g cm^{-3})	1.362	1.369	1.359	1.368
μ (mm^{-1})	0.524	0.510	0.523	0.510
F(000)	1556	1620	778	405
θ range for data collection (˚)	4.19–25.00	4.11–25.00	4.23–25.00	4.19–25.00
h,k,l range	-12:20, -13:13, -23:23	-22:20; -12:9, -22:24	-10:10, -11:11, -27:27	-9:9, -12:12, -14:10
Scan type	ω	ω	ω	ω
No. measured reflections	7559	15973	11806	6750
No. independent reflections (R_{int})	3198 (0.0427)	6610 (0.0480)	6410 (0.0211)	3318 (0.0281)
No. observed reflections, $I \geq 2\sigma(I)$	2489	4180	4829	2870
No. refined parameters	244	507	481	254
R, wR [$I \geq 2\sigma(I)$]	0.0424, 0.0863	0.0614, 0.1128	0.0474, 0.1030	0.0365, 0.0809
R, wR [all data]	0.0613, 0.0950	0.1099, 0.1293	0.0686, 0.1141	0.0453, 0.0853
Goodness of fit on F^2, S	1.014	1.046	1.108	1.045
Max., min. electron density (e $Å^{-3}$)	0.26, -0.26	0.52, -0.39	0.39, -0.36	0.21, -0.20
CCDC number	1487849	1487851	1487853	1487855

Table S2. Crystal data and details of the structure determination for **1b**−**4b**.

Compound	**1b**	**2b**	**3b**	**4b**
Formula	$C_{42}H_{34}NiN_4O_6$	$C_{44}H_{38}NiN_4O_6$	$C_{42}H_{34}NiN_4O_6$	$C_{44}H_{38}NiN_4O_6$
M_r	749.44	777.49	749.44	777.47
Colour and habit	light green, block	light green, plate	light green, block	light green, block
Crystal system, space group	monoclinic, *C*2/*c*	monoclinic, $P2_1/c$	triclinic, *P*-1	triclinic, *P*-1
Crystal dimensions (mm^3)	0.26 × 0.21 × 0.19	0.21 × 0.15 × 0.07	0.47 × 0.43 × 0.32	0.34 × 0.27 × 0.21
a (Å)	17.0425(5)	19.4580(11)	8.6936(3)	8.1086(4)
b (Å)	11.1186(3)	10.3297(4)	9.5467(5)	10.7384(5)
c (Å)	19.9944(7)	20.9294(13)	23.0920(12)	11.8404(6)
α (°)	90	90	80.119(4)	111.943(5)
β (°)	106.505(3)	112.782(7)	86.432(4)	90.941(4)
γ (°)	90	90	74.779(4)	100.757(4)
V ($Å^3$)	3632.6(2)	3878.5(4)	1821.58(15)	935.28(8)
Z	4	4	2	1
D_{calc} (g cm^{-3})	1.370	1.331	1.366	1.380
μ (mm^{-1})	0.589	0.554	0.587	0.574
F(000)	1560	1624	780	406
θ range for data collection (°)	4.16–25.00	4.08–25.00	4.25–25.00	4.25–25.00
h,*k*,*l* range	-20:18, -13:13, -19:23	-23:23; -12:12, -24:24	-7:10, -11:11, -27:25	-8:9, -12:11, -14:13
Scan type	ω	ω	ω	ω
No. measured reflections	7516	29967	13226	6743
No. independent reflections (R_{int})	3177 (0.0204)	6802 (0.1425)	6380 (0.0283)	3261 (0.0221)
No. observed reflections, $I \geq 2\sigma(I)$	2831	3465	4624	3026
No. refined parameters	244	501	481	254
R, w*R* [$I \geq 2\sigma(I)$]	0.0295, 0.0708	0.0859, 0.1226	0.0428, 0.0938	0.0298, 0.0847
R, w*R* [all data]	0.0351, 0.0734	0.1800, 0.1517	0.0659, 0.1044	0.0334, 0.0861
Goodness of fit on F^2, *S*	1.009	1.069	1.037	1.196
Max., min. electron density (e $Å^{-3}$)	0.26, -0.20	0.41, -0.25	0.32, -0.35	0.19, -0.29
CCDC number	1487850	1487852	1487854	1487856

Table S3. Crystal data and details of the structure determination for **5**−**7**.

Compound	**5**	**6**	**7**
Formula	$C_{22}H_{14}CoF_{12}N_4O_6$	$C_{24}H_{18}CoF_{12}N_4O_6$	$C_{24}H_{18}CoF_{12}N_4O_6$
M_r	717.3	745.35	745.35
Colour and habit	orange, prism	orange, prism	orange, prism
Crystal system, space group	triclinic, *P*-1	triclinic, *P*-1	triclinic, *P*-1
Crystal dimensions (mm^3)	0.19 × 0.09 × 0.06	0.63 × 0.25 × 0.22	0.39 × 0.31 × 0.18
a (Å)	7.0829(7)	6.6893(4)	9.2041(5)
b (Å)	10.0466(14)	11.2108(10)	11.8190(5)
c (Å)	10.2978(13)	11.2507(10)	14.2346(7)
α (˚)	66.775(13)	117.658(9)	97.036(4)
β (˚)	79.294(9)	96.963(6)	103.584(4)
γ (˚)	84.324(10)	91.225(6)	90.449(4)
V ($Å^3$)	661.41(14)	738.90(10)	1492.76(13)
Z	1	1	2
D_{calc} (g cm^{-3})	1.801	1.675	1.658
μ (mm^{-1})	0.781	0.702	0.695
F(000)	357	373	746
θ range for data collection (˚)	4.11–25.00	4.25–25.00	4.15–25.00
h,*k*,*l* range	-8:7; -11:9, -12:12	-7:6; -13:10, -13:13	-10:10, -14:13, -15:16
Scan type	ω	ω	ω
No. measured reflections	4630	4586	9649
No. independent reflections (R_{int})	2319 (0.0481)	2578 (0.0243)	5209 (0.0243)
No. observed reflections, $I \geq 2\sigma(I)$	1660	2282	4053
No. refined parameters	205	244	435
R, w*R* [$I \geq 2\sigma(I)$]	0.0650, 0.1405	0.0421, 0.1152	0.0550, 0.1484
R, w*R* [all data]	0.0948, 0.1544	0.0494, 0.1213	0.0716, 0.1596
Goodness of fit on F^2, *S*	1.035	1.099	1.020
Max., min. electron density (e $Å^{-3}$)	0.35, -0.31	0.42, -0.29	0.92, -0.57
CCDC number	1487857	1487858	1487859

Table S4. Selected bond distances (Å) and angles (˚) for **1a**−**4a**.

	1a	**2a**	**3a**	**4a**
Bond distances				
Co1–O1	2.044(1)	2.036(2)	2.060(2)	2.030(1)
Co1–O2	2.010(1)	2.109(2)	2.033(2)	2.023(1)
Co1–N1	2.207(2)	2.182(3)	2.182(2)	2.219(2)
Co2–O4		2.030(2)	2.062(2)	
Co2–O5		2.080(3)	2.026(2)	
Co2–N3		2.151(3)	2.182(2)	
Bond angles				
O1–Co1–O2^{i}	89.98(6)	90.00(9)	90.55(7)	91.16(5)
O1–Co1–O2	90.02(6)	90.00(9)	89.45(7)	88.84(5)
O1–Co1–N1	93.03(7)	88.5(1)	93.78(7)	91.26(5)
O2–Co1–N1	90.00(7)	89.4(1)	91.17(7)	85.89(6)
O1–Co1–N1^{i}	86.97(7)	91.5(1)	86.22(7)	88.74(5)
O2–Co1–N1^{i}	90.00(7)	90.6(1)	88.83(7)	94.11(6)
O4–Co2–O5		90.3(1)	88.99(7)	
O4–Co2–O5^{ii}		89.7(1)	91.01(7)	
O5–Co2–N3^{ii}		93.9(1)	92.96(7)	
O4–Co2–N3^{ii}		91.1(1)	91.90(7)	
O5–Co2–N3		86.1(1)	87.04(7)	
O4–Co2–N3		88.9(1)	88.10(7)	

Symmetry codes (i): -x+1/2, -y+1/2, -z+1 (**1a**), –x, -y+1, -z (**2a**), -x, -y, -z+1 (**3a**), -x+1, -y+1, -z (**4a**); (ii): -x+1, -y, -z+1 (**2a**), -x+1, -y+1, -z (**3a**).

Table S5. Selected bond distances (Å) and angles (˚) for **1b**−**4b**.

	1b	**2b**	**3b**	**4b**
Bond distances				
Ni1–O1	2.030(1)	2.025(3)	2.039(2)	2.010(1)
Ni1–O2	1.997(1)	2.077(3)	2.019(2)	2.011(1)
Ni1–N1	2.137(1)	2.129(4)	2.119(2)	2.161(1)
Ni2–O4		2.019(4)	2.048(2)	
Ni2–O5		2.052(3)	2.006(2)	
Ni2–N3		2.110(5)	2.118(2)	
Bond angles				
O1–Ni1–O2^{i}	88.59(5)	87.7(1)	89.05(6)	89.50(5)
O1–Ni1–O2	91.41(5)	92.3(1)	90.95(6)	90.50(5)
O1–Ni1–N1	92.64(5)	88.9(2)	93.17(7)	91.09(6)
O2–Ni1–N1	89.53(5)	89.9(1)	90.64(7)	86.52(5)
O1–Ni1–N1^{i}	87.36(5)	91.1(2)	86.83(7)	88.91(5)
O2–Ni1–N1^{i}	90.47(5)	90.1(1)	89.36(7)	93.48(5)
O4–Ni2–O5		91.7(2)	90.44(6)	
O4–Ni2–O5^{ii}		88.3(2)	89.56(6)	
O5–Ni2–N3^{ii}		92.2(2)	92.06(7)	
O4–Ni2–N3^{ii}		90.3(2)	91.09(7)	
O5–Ni2–N3		87.8(2)	87.94(7)	
O4–Ni2–N3		89.7(2)	88.91(7)	

Symmetry codes (i): -x+1/2, -y+1/2, -z+1 (**1b**), –x, -y+1, -z (**2b**), -x, -y, -z+1 (**3b**), –x+1, -y+1, -z (**4b**); (ii): -x+1, -y, -z+1 (**2b**), -x+1, -y+1, -z (**3b**).

Table S6. Selected bond distances (Å) and angles (°) for **5**−**7**.

	5	**6**	**7**
Co1–O1	2.043(3)	2.075(2)	2.059(3)
Co1–O2	2.091(3)	2.066(2)	2.035(2)
Co1–N1	2.182(4)	2.174(2)	2.172(3)
Co2–O4			2.046(2)
Co2–O5			2.058(2)
Co2–N3			2.169(3)
O1–Co1–O2^{i}	92.4(1)	91.78(7)	91.0(1)
O1–Co1–O2	87.6(1)	88.22(7)	89.0(1)
O1–Co1–N1	90.2(1)	89.53(8)	84.9(1)
O2–Co1–N1	91.8(1)	91.23(8)	90.8(1)
O1–Co1–N1^{i}	89.9(1)	90.47(8)	95.1(1)
O2–Co1–N1^{i}	88.2(1)	88.77(8)	89.2(1)
O4–Co2–O5			89.3(1)
O4–Co2–O5^{ii}			90.7(1)
O5–Co2–N3^{ii}			94.3(1)
O4–Co2–N3^{ii}			88.2(1)
O5–Co2–N3			85.7(1)
O4–Co2–N3			91.8(1)

Symmetry codes (i): -x, -y, -z (**5**), -x+1, -y, -z+1 (**6**), –x+1, -y, -z (**7**); (ii): -x-1, -y-1, -z+1 (**7**).

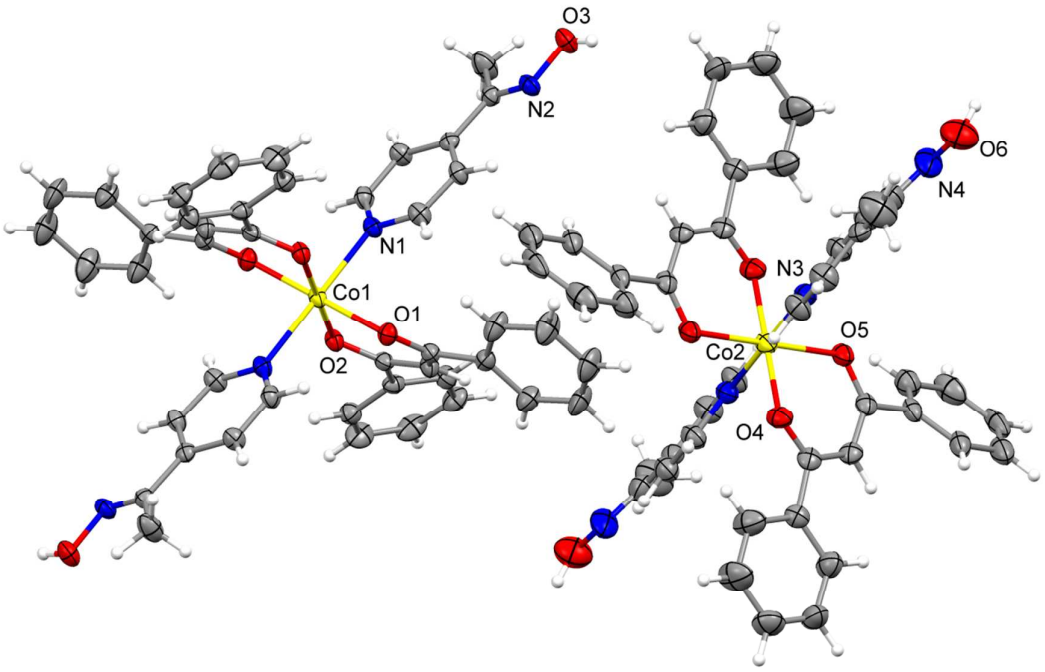

Figure S1. ORTEP-style plot of $[Co(dbm)_2(4\text{-Meoxpy})_2]$ (**2a**) with partial labeling scheme, showing both crystallographically independent molecules. Thermal ellipsoids are drawn at 40% probability level at 200(2) K

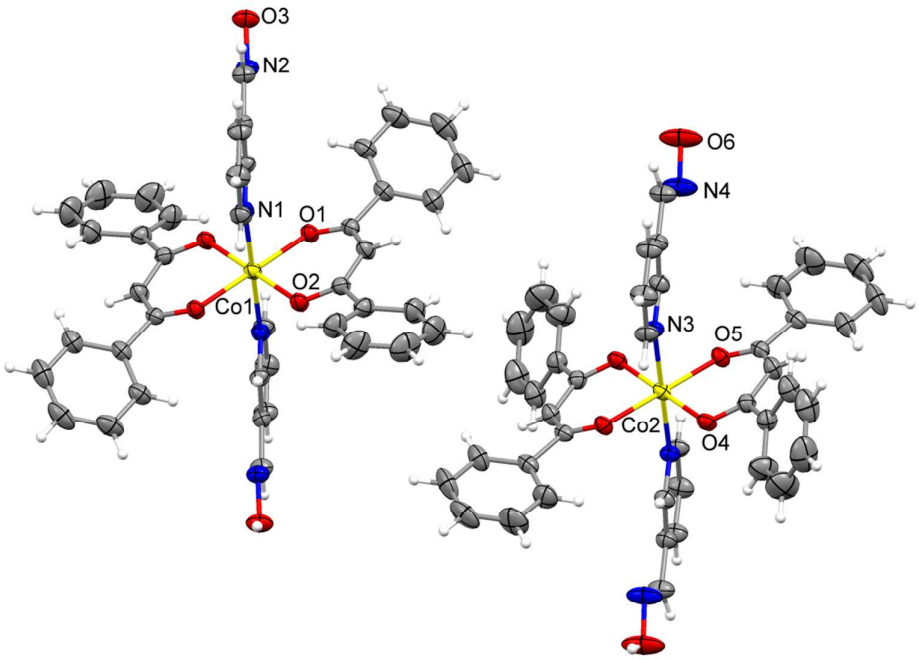

Figure S2. ORTEP-style plot of $[Co(dbm)_2(3\text{-Hoxpy})_2]$ (**3a**) with partial labeling scheme, showing both crystallographically independent molecules. Thermal ellipsoids are drawn at 40% probability level at 296(2) K.

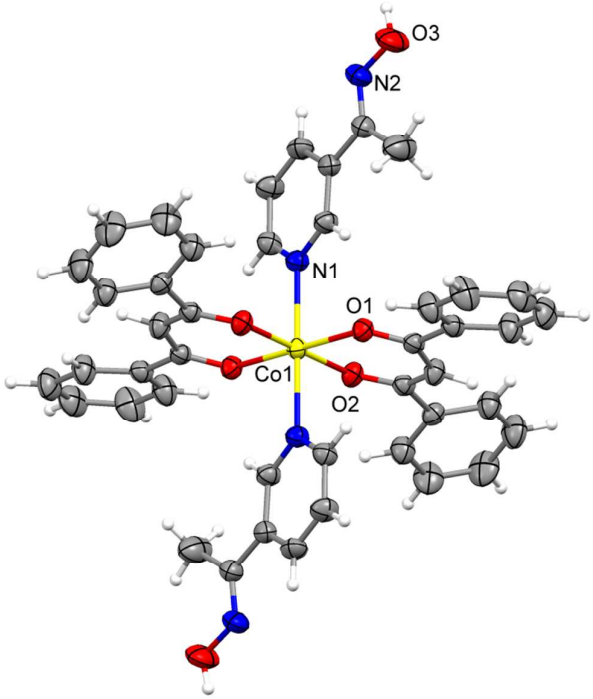

Figure S3. ORTEP-style plot of $[Co(dbm)_2(3\text{-}Meoxpy)_2]$ (**4a**) with partial labeling scheme. Thermal ellipsoids are drawn at 40% probability level at 296(2) K.

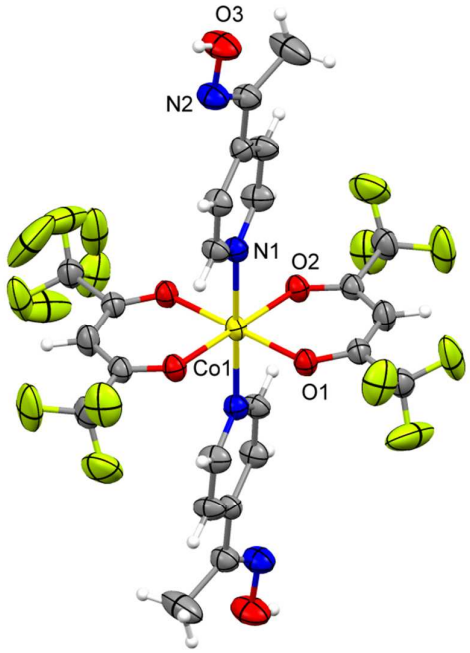

Figure S4. ORTEP-style plot of $[Co(hfac)_2(4\text{-}Meoxpy)_2]$ (**6**) with partial labeling scheme. Thermal ellipsoids are drawn at 40% probability level at 296(2) K.

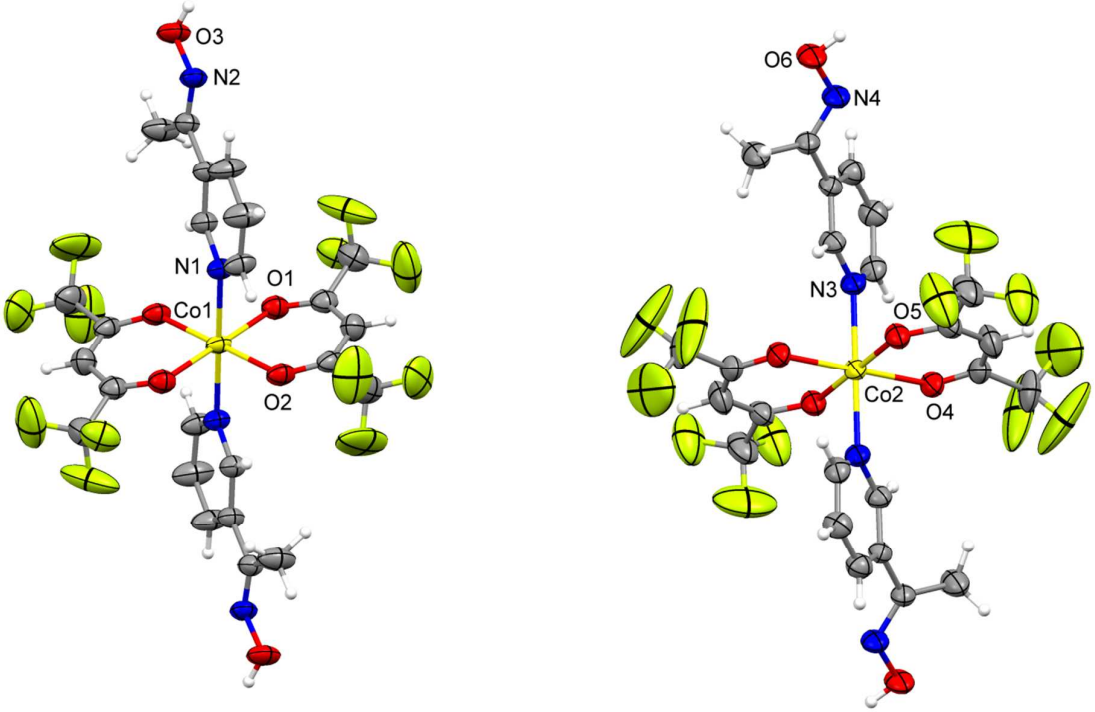

Figure S5. ORTEP-style plot of $[Co(hfac)_2(3\text{-}Meoxpy)_2]$ (**7**) with partial labeling scheme, showing both crystallographically independent molecules. Thermal ellipsoids are drawn at 40% probability level at 296(2) K.

2. Powder X-ray crystallography

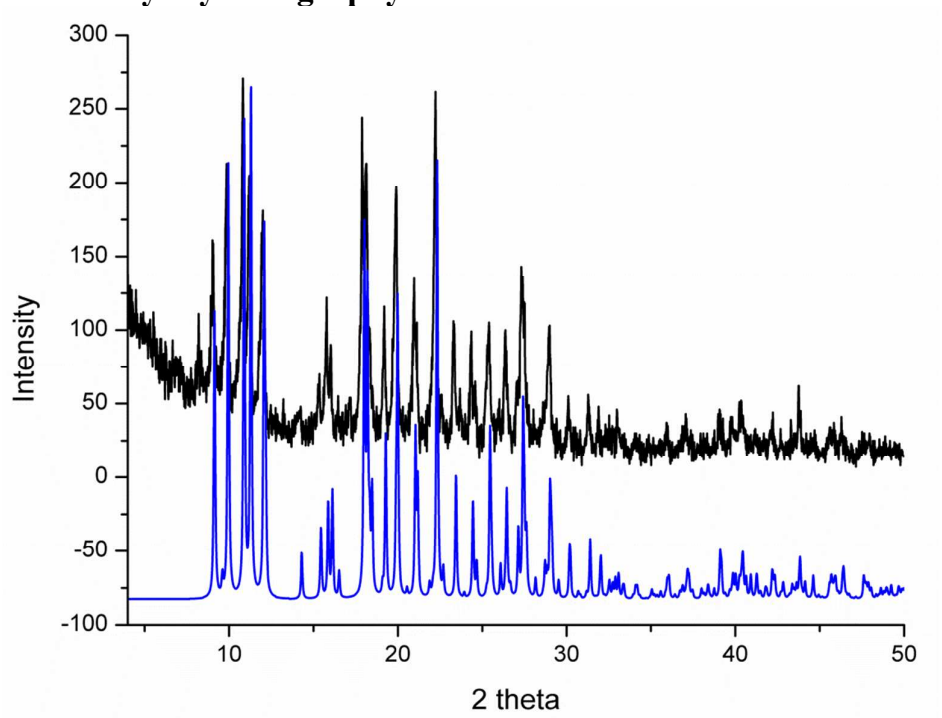

Figure S6. Experimental (**black**) and calculated (**blue**) PXRD traces of $[Co(dbm)_2(4\text{-}Hoxpy)_2]$ (**1a**)

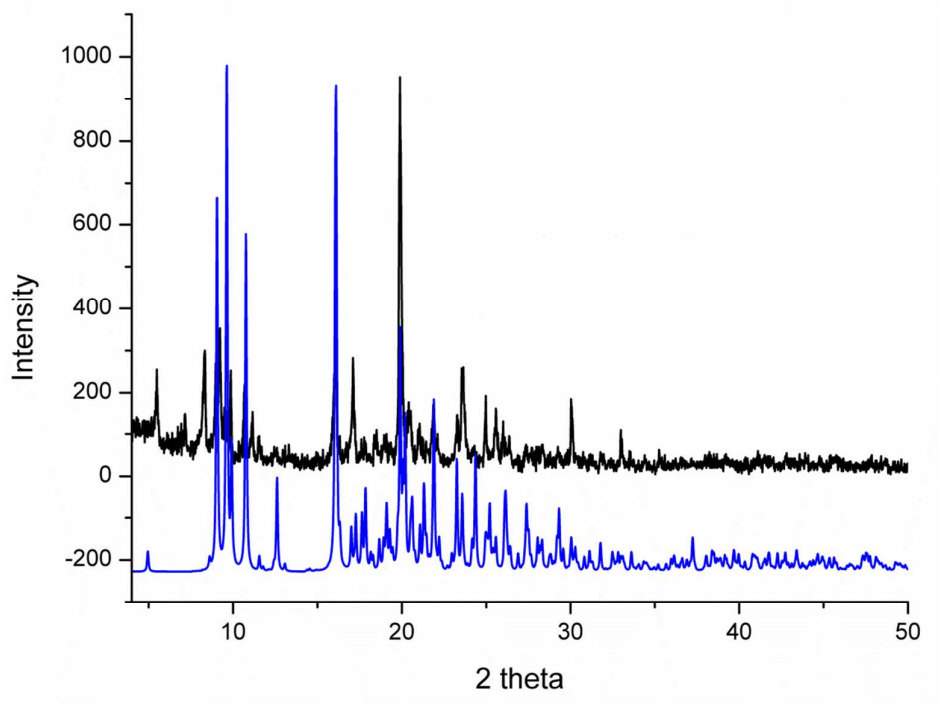

Figure S7. Experimental (**black**) and calculated (**blue**) PXRD traces of $[Co(dbm)_2(4\text{-}Meoxpy)_2]$ (**2a**)

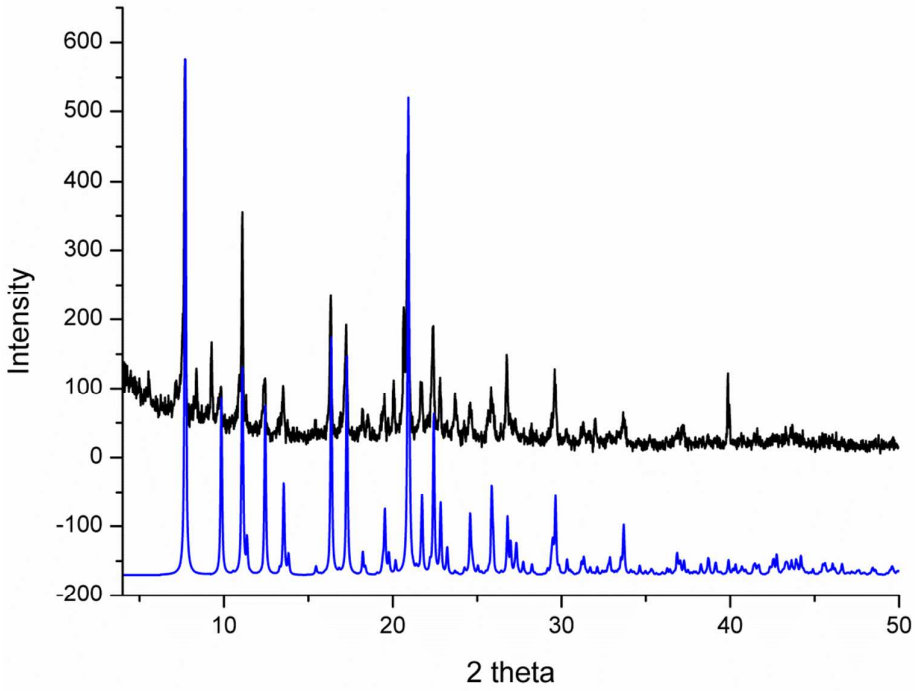

Figure S8. Experimental (**black**) and calculated (**blue**) PXRD traces of $[Co(dbm)_2(3\text{-}Hoxpy)_2]$ (**3a**)

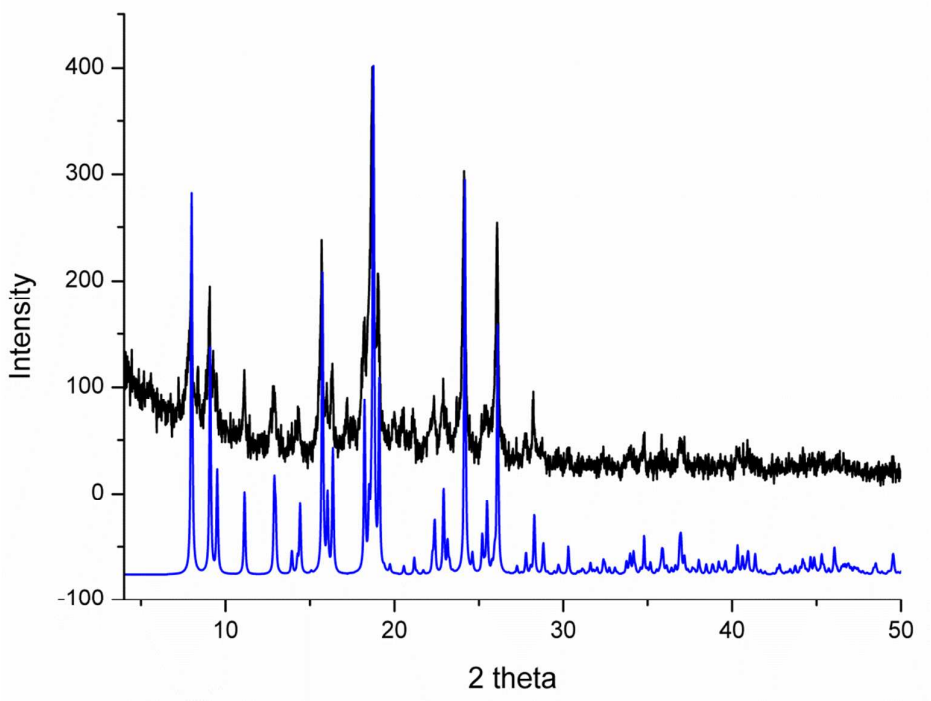

Figure S9. Experimental (**black**) and calculated (**blue**) PXRD traces of $[Co(dbm)_2(3\text{-}Meoxpy)_2]$ (**4a**)

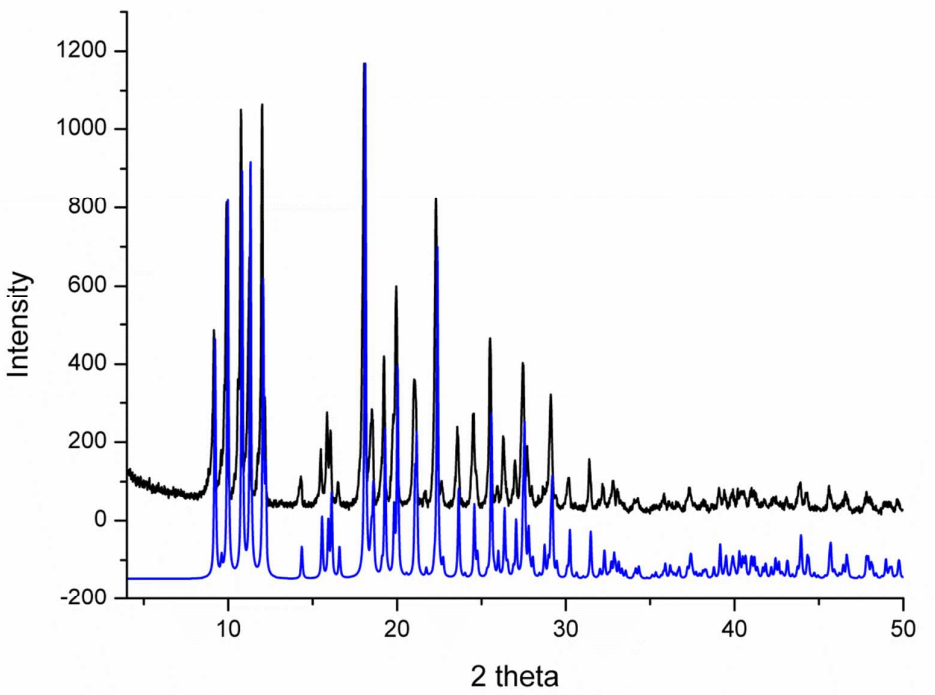

Figure S10. Experimental (**black**) and calculated (**blue**) PXRD traces of $[Ni(dbm)_2(4\text{-}Hoxpy)_2]$ (**1b**)

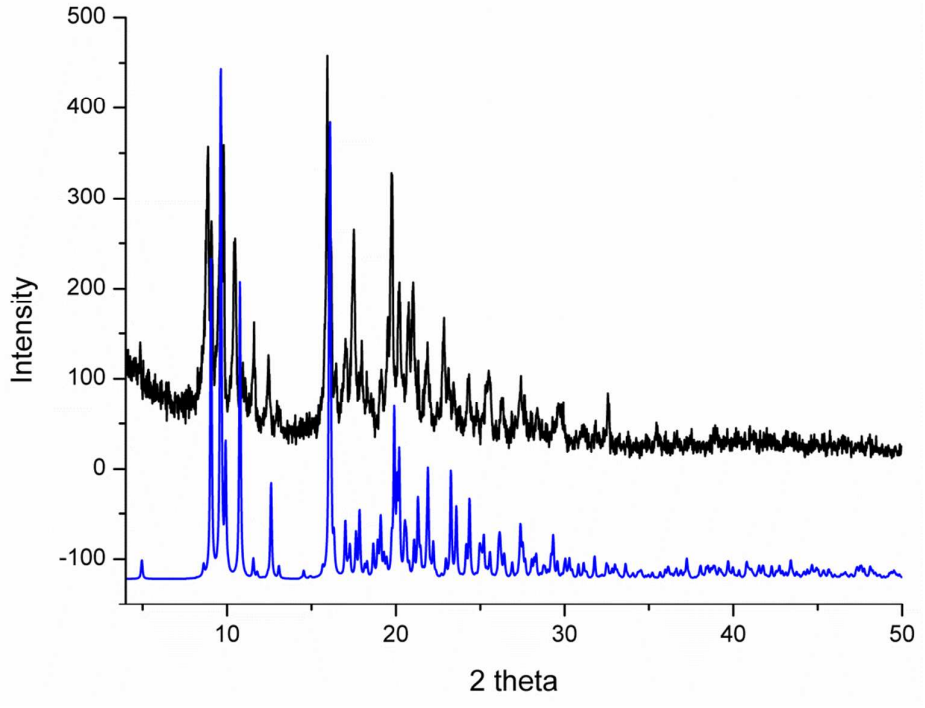

Figure S11. Experimental (**black**) and calculated (**blue**) PXRD traces of $[Ni(dbm)_2(4\text{-}Meoxpy)_2]$ (**2b**)

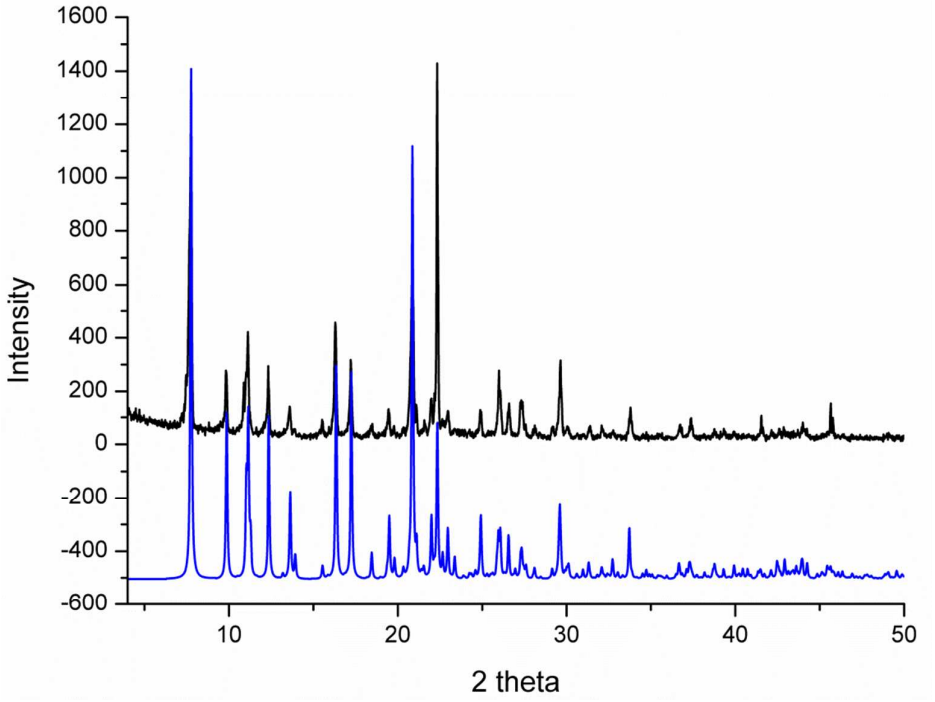

Figure S12. Experimental (**black**) and calculated (**blue**) PXRD traces of[$Ni(dbm)_2(3\text{-}Hoxpy)_2$] (**3b**)

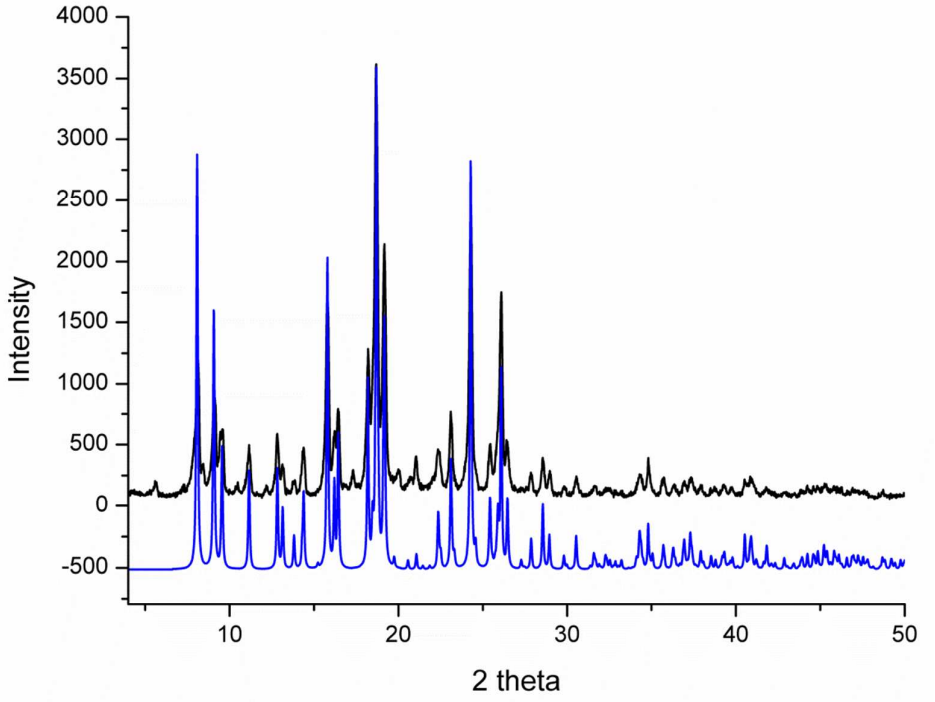

Figure S13. Experimental (**black**) and calculated (**blue**) PXRD traces of [$Ni(dbm)_2(3\text{-}Meoxpy)_2$] (**4b**)

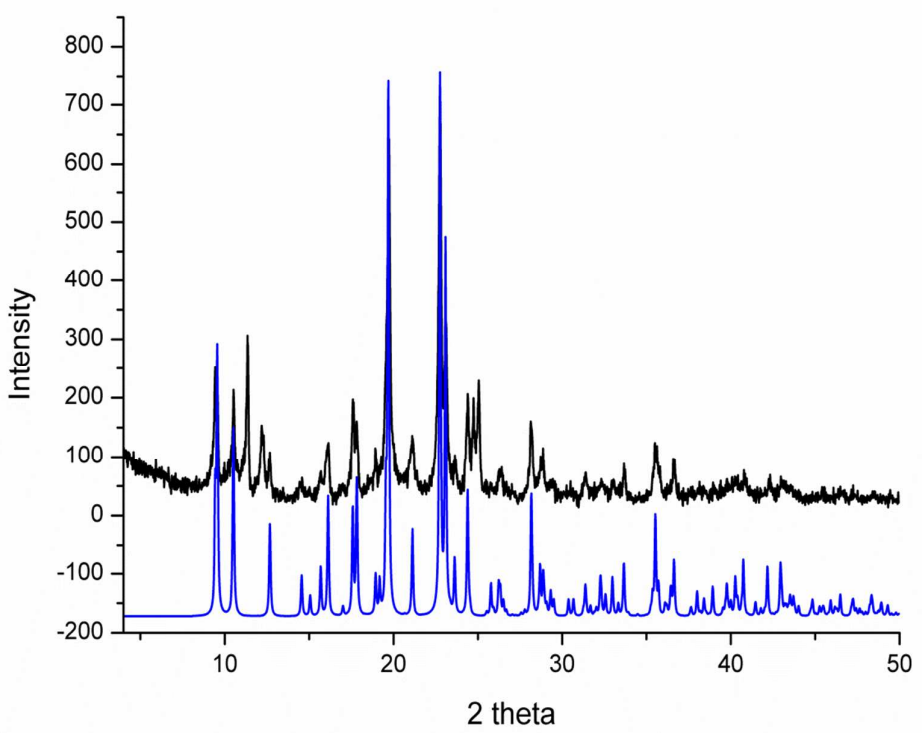

Figure S14. Experimental (**black**) and calculated (**blue**) PXRD traces of $[Co(hfac)_2(4\text{-}Hoxpy)_2]$ (**5**)

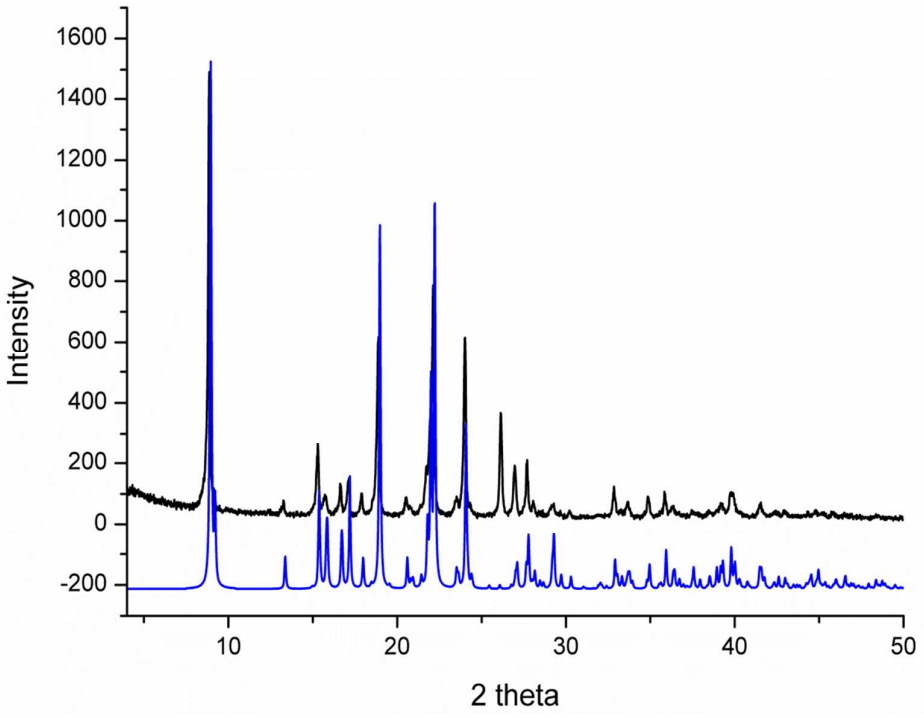

Figure S15. Experimental (**black**) and calculated (**blue**) PXRD traces of $[Co(hfac)_2(4\text{-}Meoxpy)_2]$ (**6**)

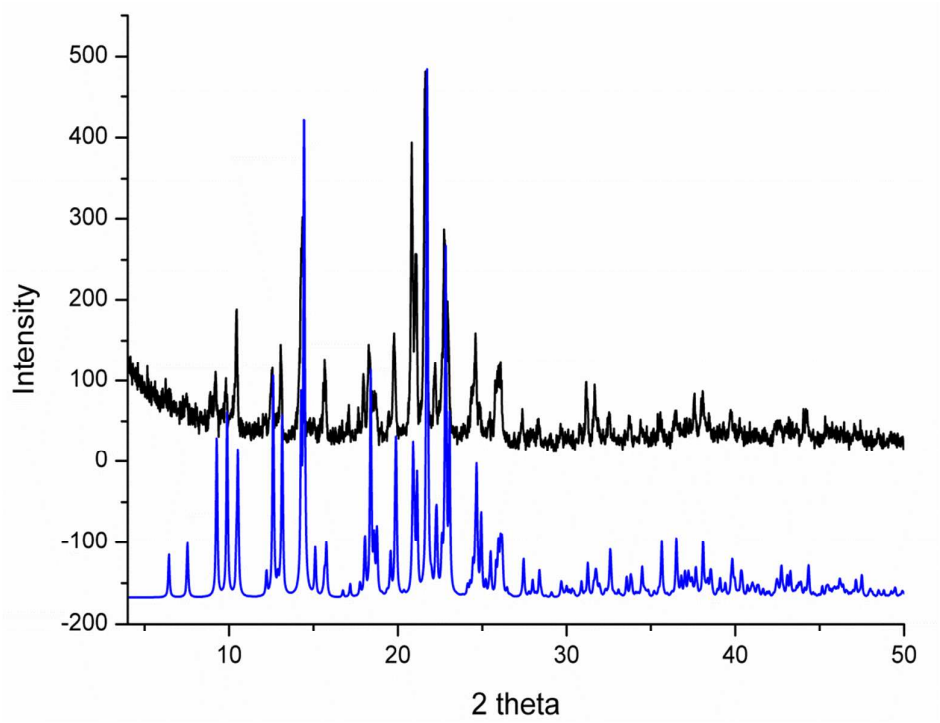

Figure S16. Experimental (**black**) and calculated (**blue**) PXRD traces of [Co(hfac)$_2$(3-Meoxpy)$_2$] (**7**)

3. IR spectroscopic and thermal analysis

$[Co(dbm)_2(4\text{-}Hoxpy)_2]$ (1a)

FT-IR (KBr, cm^{-1}): 3139 (m), 3062 (m), 2972 (m), 2881 (m), 2753 (m), 2603 (w), 2344 (w), 1964 (w), 1916 (w), 1812 (w), 1761 (w), 1591 (s), 1544 (s), 1479 (s), 1442 (s), 1399(s), 1329(m), 1307 (s), 1226(s), 1181 (s), 1133 (m), 1092 (m), 1073 (m), 1056 (m), 1022 (m), 1012 (m), 994 (s), 936 (m), 884 (m), 851 (m), 822 (m), 798 (m), 780 (m), 740 (m), 721 (s), 692 (s), 667 (m), 651 (s), 626 (m), 540 (s), 454 (m).

$[Co(dbm)_2(4\text{-}Meoxpy)_2]$ (2a)

FT-IR (KBr, cm^{-1}): 3381 (m), 3058 (w), 2924 (w), 2853 (w), 2345 (w), 1955 (w), 1660 (w), 1594 (s), 1547 (s), 1524 (s), 1480 (s), 1455 (s), 1441 (m), 1400 (s), 1306 (s), 1232 (m), 1183 (m), 1163 (w), 1131 (w), 1095 (w), 1071 (w), 1060 (m), 1022 (m), 1001 (m), 940 (m), 868 (w), 831 (m), 810 (w), 788 (m), 747 (m), 724 (m), 689 (m), 669 (m), 657 (m), 626 (m), 569 (w), 522 (m).

$[Co(dbm)_2(3\text{-}Hoxpy)_2]$ (3a)

FT-IR (KBr, cm^{-1}): 3854 (w), 3271 (m), 3063 (w), 2979 (w), 2924 (w), 2875 (w), 2738 (w), 1953 (w), 1908 (w), 1814 (w), 1619 (w), 1592 (s), 1546 (s), 1519 (s), 1479 (s), 1458 (s), 1427 (m), 1401 (s), 1328 (m), 1299 (s), 1224 (m), 1191 (m), 1181 (m), 1130 (w), 1105 (w), 1072 (m), 1058 (m), 1022 (m), 1000 (w), 977 (m), 940 (m), 885 (m), 809 (w), 785 (w), 774 (w), 724 (m), 702 (m), 692 (m), 670 (m), 643 (w), 624 (m), 534 (m).

$[Co(dbm)_2(3\text{-}Meoxpy)_2]$ (4a)

FT-IR (KBr, cm^{-1}): 3301(m), 3257 (m), 3143 (w), 3105 (w), 3065 (w), 3039 (w), 2925 (w), 2345 (w), 1945 (w), 1894 (w), 1807 (w), 1753 (w), 1593 (s), 1546 (s), 1512 (s), 1475 (s), 1459 (s), 1442 (m), 1416 (s), 1328 (m), 1308 (m), 1285 (m), 1220 (m), 1201 (m), 1180 (m), 1162 (w), 1132 (m), 1106 (w), 1092 (w), 1072 (m), 1058 (m), 1022 (m), 1005 (m), 968 (w), 929 (m), 846 (w), 816 (m), 782 (m), 748 (m), 716 (m), 704 (m), 683 (m), 637 (w), 625 (m), 528 (m).

$[Ni(dbm)_2(4\text{-}Hoxpy)_2]$ (1b)

FT-IR (KBr, cm^{-1}): 3437 (w), 3136 (w), 3065 (w), 2969 (w), 2924 (w), 2878 (w), 2752 (w), 2605 (w), 2479 (w), 2321 (w), 1964 (w), 1945 (w), 1916 (w), 1900 (w), 1812 (w), 1761 (w), 1592 (m), 1547 (s), 1518 (s), 1480 (s), 1454 (m), 1443 (m), 1404 (s), 1329 (w), 1307 (m), 1295 (m), 1226 (m), 1181 (m), 1134 (w), 1093 (w), 1074 (w), 1056 (w), 1018 (m), 995 (m), 983 (m), 935 (m), 885 (m), 872 (w), 854 (w), 822 (m), 813 (m), 799 (w), 779 (m), 740 (w), 722 (m), 693 (m), 667 (w), 654 (m), 633 (m), 541 (m), 455 (m).

$[Ni(dbm)_2(4\text{-}Meoxpy)_2]$ (2b)

FT-IR (KBr, cm^{-1}): 3380 (m), 3276 (m), 3059 (w), 2924 (w), 2854 (w), 2575 (w), 1953 (w), 1894 (w), 1810 (w), 1594 (s), 1550 (s), 1522 (s), 1480 (s), 1455 (s), 1407 (s), 1304 (m), 1220 (m), 1181 (w), 1158 (w), 1133 (w), 1095 (w), 1072 (w), 1057 (w), 1012 (m), 940 (m), 831

(m), 809 (w), 785 (w), 745 (w), 725 (m), 692 (m), 669 (w), 660 (w), 632 (m), 569 (w), 533 (w).

[Ni(dbm)$_2$(3-Hoxpy)$_2$] (3b)

FT-IR (KBr, cm^{-1}): 3236 (m), 3066 (m), 2981 (w), 2925 (w), 2880 (w), 2738 (w), 2596 (w), 2345 (w), 1953 (w), 1909 (w), 1848 (w), 1813 (w), 1762 (w), 1620 (w), 1593 (s), 1549 (s), 1519 (s), 1480 (s), 1460 (s), 1405 (s), 1327 (w), 1299 (s), 1225 (m), 1190 (w), 1181 (w), 1131 (w), 1107 (w), 1073 (m), 1057 (m), 1022 (m), 1000 (w), 978 (m), 956 (w), 941 (m), 887 (m), 846 (w), 809 (m), 785 (m), 773 (m), 726 (m), 702 (m), 693 (m), 671 (m), 647 (w), 631 (m), 535 (m), 455 (w).

[Ni(dbm)$_2$(3-Meoxpy)$_2$] (4b)

FT-IR (KBr, cm^{-1}): 3296 (m), 3255 (m), 3143 (w), 3106 (w), 3066 (w), 3042 (w), 2927 (w), 2641 (w), 2568 (w), 1945 (w), 1898 (w), 1879 (w), 1808 (w), 1755 (w), 1642 (w), 1619 (w), 1594 (s), 1548 (s), 1475 (s), 1459 (s), 1442 (m), 1418 (s), 1372 (m), 1327 (m), 1307 (m), 1284 (m), 1220 (m), 1201 (m), 1180 (w), 1162 (w), 1153 (w), 1132 (m), 1109 (w), 1093 (w), 1072 (w), 1065 (m), 1058 (m), 1048 (w), 1022 (m), 1005 (m), 969 (w), 961 (w), 930 (m), 846 (w), 817 (m), 782 (m), 745 (m), 717 (s), 703 (m), 690 (m), 682 (m), 635 (m), 527 (m), 455 (w).

[Co(hfac)$_2$(4-Hoxpy)$_2$] (5)

FT-IR (KBr, cm^{-1}): 3310 (m), 2925 (w), 2855 (w), 1645 (s), 1611 (m), 1554 (m), 1526 (m), 1499 (m), 1417 (m), 1377 (w), 1339 (w), 1328 (w), 1309 (w), 1256 (s), 1221 (s), 1197 (s), 1150 (s), 1137 (s), 1094 (m), 1017 (m), 943 (m), 835 (m), 796 (m), 744 (w), 670 (m), 588 (m), 575 (w).

[Co(hfac)$_2$(4-Meoxpy)$_2$] (6)

FT-IR (KBr, cm^{-1}): 3314 (m), 3266 (m), 2925 (w), 2855 (w), 2467 (w), 1962 (w), 1645 (s), 1610 (m), 1554 (m), 1526 (m), 1499 (m), 1417 (m), 1376 (w), 1339 (w), 1327 (w), 1308 (w), 1256 (s), 1220 (s), 1197 (s), 1149 (s), 1137 (s), 1093 (m), 1067 (w), 1017 (m), 942 (m), 874 (w), 835 (m), 811 (w), 796 (m), 744 (w), 670 (m), 652 (w), 588 (m), 575 (w), 528 (w), 484 (w).

[Co(hfac)$_2$(3-Meoxpy)$_2$] (7)

FT-IR (KBr, cm^{-1}): 3313 (m), 3268 (m), 3143 (w), 3111 (w), 3081 (w), 2933 (w), 1641 (s), 1600 (m), 1558 (m), 1531 (m), 1494 (m), 1423 (w), 1413 (w), 1374 (w), 1335 (w), 1314 (w), 1260 (s), 1205 (s), 1146 (s), 1099 (m), 1052 (w), 1005 (m), 930 (m), 812 (m), 804 (m), 768 (w), 745 (w), 703 (m), 679 (m), 669 (m), 645 (w), 588 (m), 529 (w).

4. Molecular electrostatic potential maps

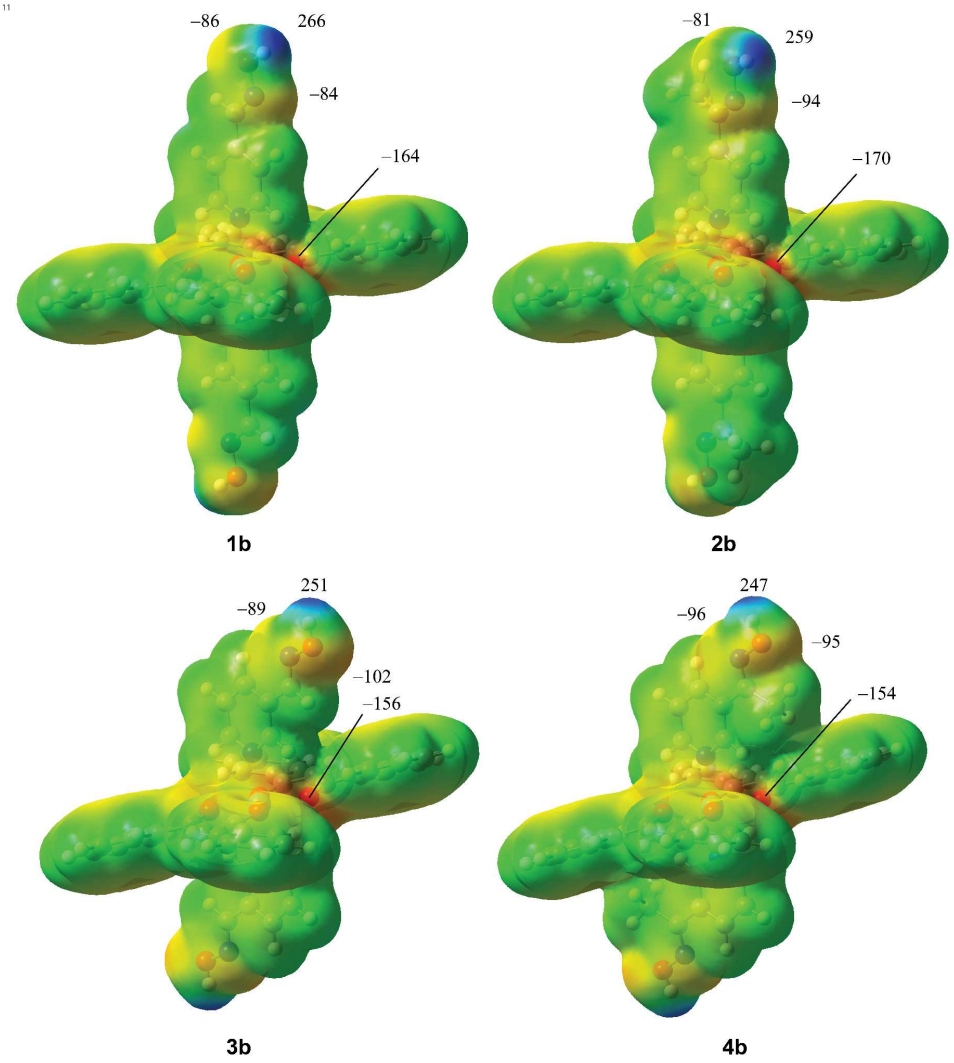

Figure S17. Electrostatic potential mapped on the 0.002 a.u. isodensity surface for all dbm-based complexes of Ni(II) calculated at the B3LYP-D3/def2-TZVP level of theory. Color range: –170 (red) to 266 kJ/mol (blue).

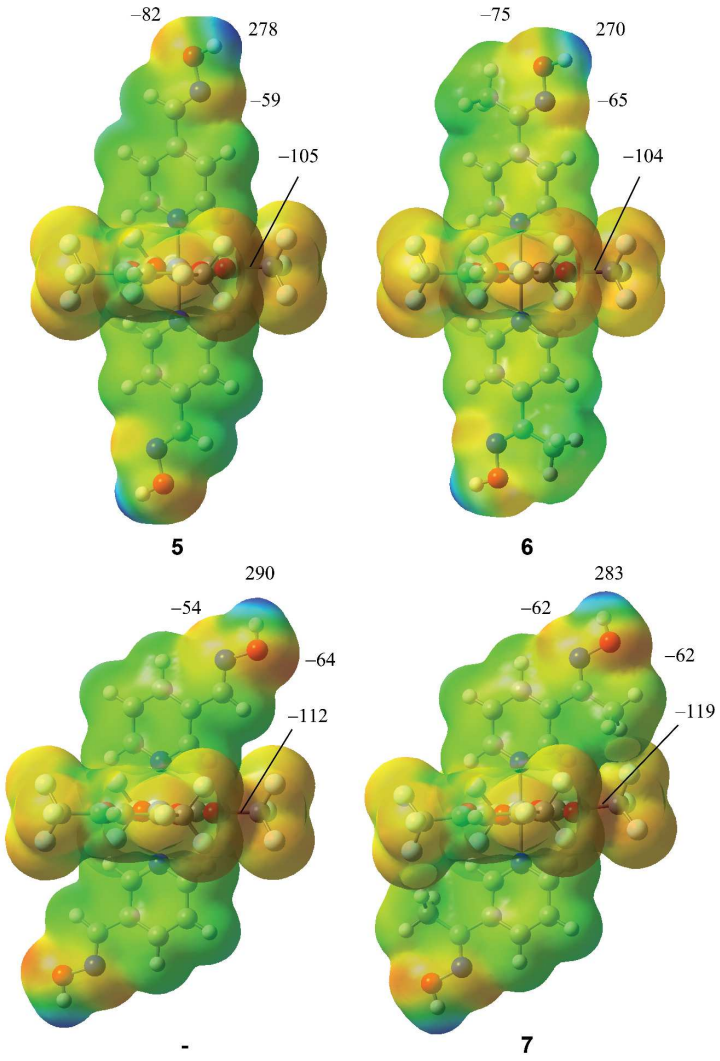

Figure S18. Electrostatic potential mapped on the 0.002 a.u. isodensity surface for all hfac-based complexes of Co(II) calculated at the B3LYP-D3/def2-TZVP level of theory. Color range: –119 (red) to 290 kJ/mol (blue). Compound $[Co(hfac)_2(3\text{-Hoxpy})_2]$ was added for the comparison purposes.

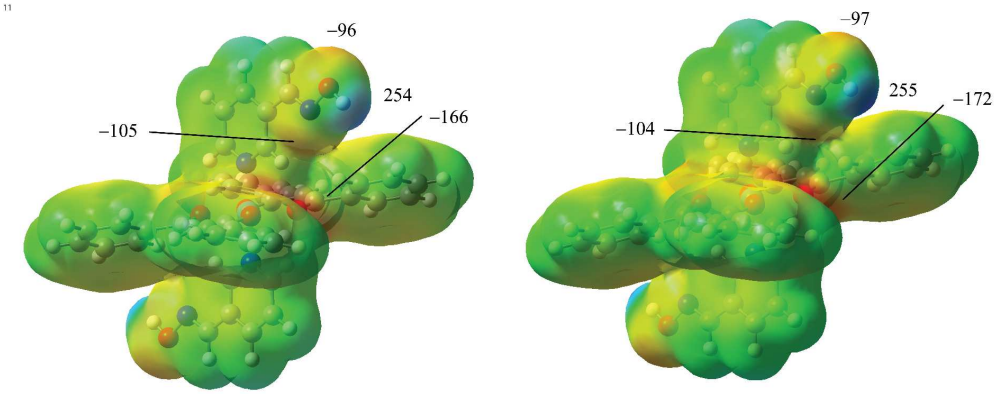

3a **3b**

Figure S19. Electrostatic potential mapped on the 0.002 a.u. isodensity surface for the less stable conformers of complexes **3a** (Co) and **3b** (Ni), color range: –172 (red) to 254 kJ/mol (blue). These two geometries correspond to the conformers determined in the crystal structures of compounds **3a** and **3b** and have a different orientation of the oxime groups than in their counterparts represented in other Figures. Although values of the electrostatic potential on N(oxime) and O(acac) are more negative in less stable conformers of **3a** (**3b**), the electrostatic potential differences stay almost the same, 61 and 68 kJ/mol, respectively.

5. Hirshfeld surface analysis

The Hirshfeld surface analysis based on 2D fingerprints examination provided us with further information regarding the crystal packing. It clearly showed that dominant interactions (pair of spikes with small d_i and d_e values) are not necessarily related to the same type of contacts. In the 2D fingerprints of hfac-containing complexes (**5**–**7**) and complexes **4a** (**4b**) the spikes belong to N(oxime)···H contacts of the oxime···oxime dimers. In all other complexes these spikes belong to O(acac)···H contacts of the O–H···O(acac) dimers.

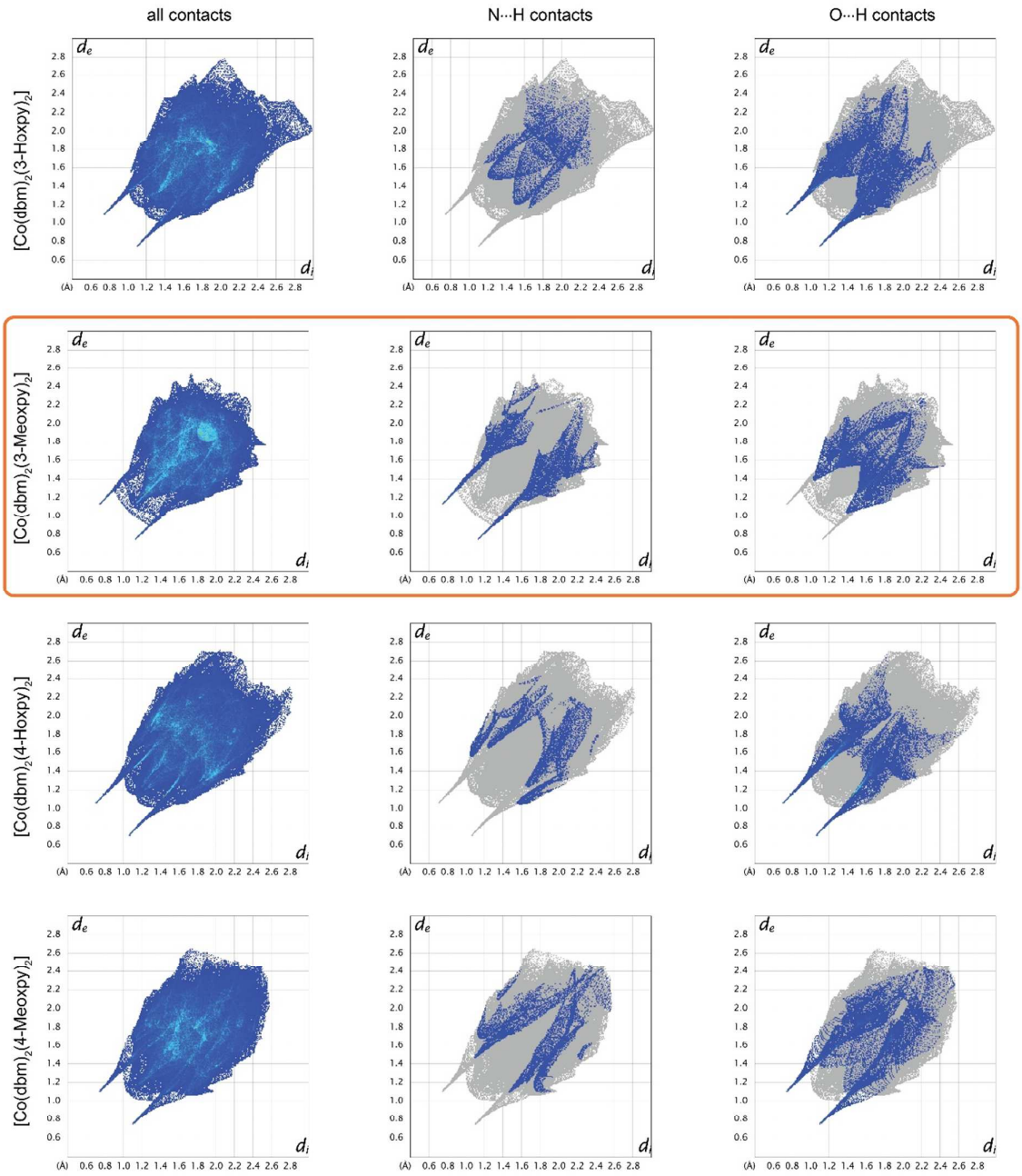

Figure S20. Fingerprint plot for Co(II) complexes with dbm ligand resolved into N···H and O···H contacts. The orange rounded rectangular marks the complex **4a** with O–H···N interaction.

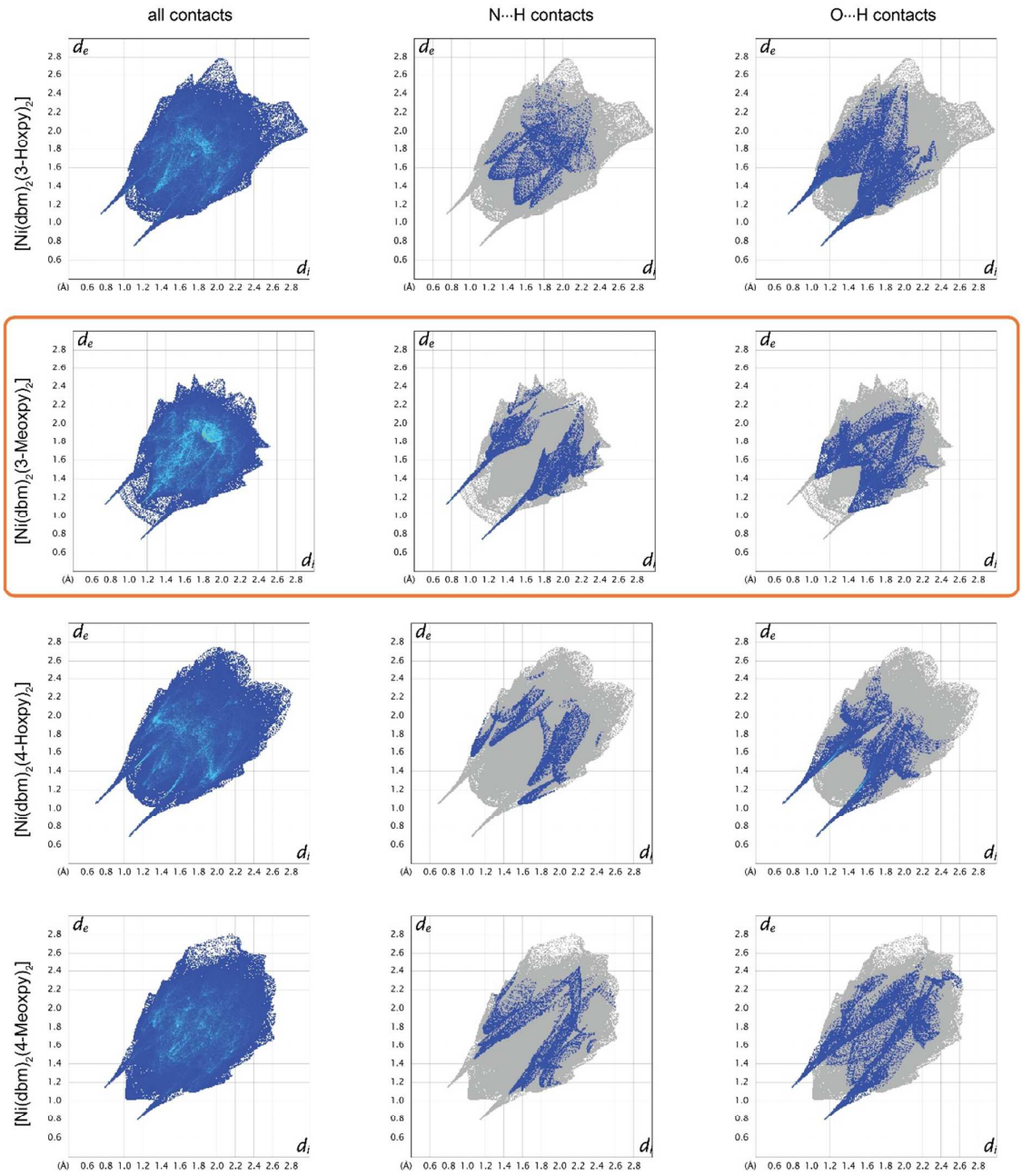

Figure S21. Fingerprint plot for Ni(II) complexes with dbm ligand resolved into N···H and O···H contacts. The orange rounded rectangular marks the complex **4b** with O–H···N interaction.

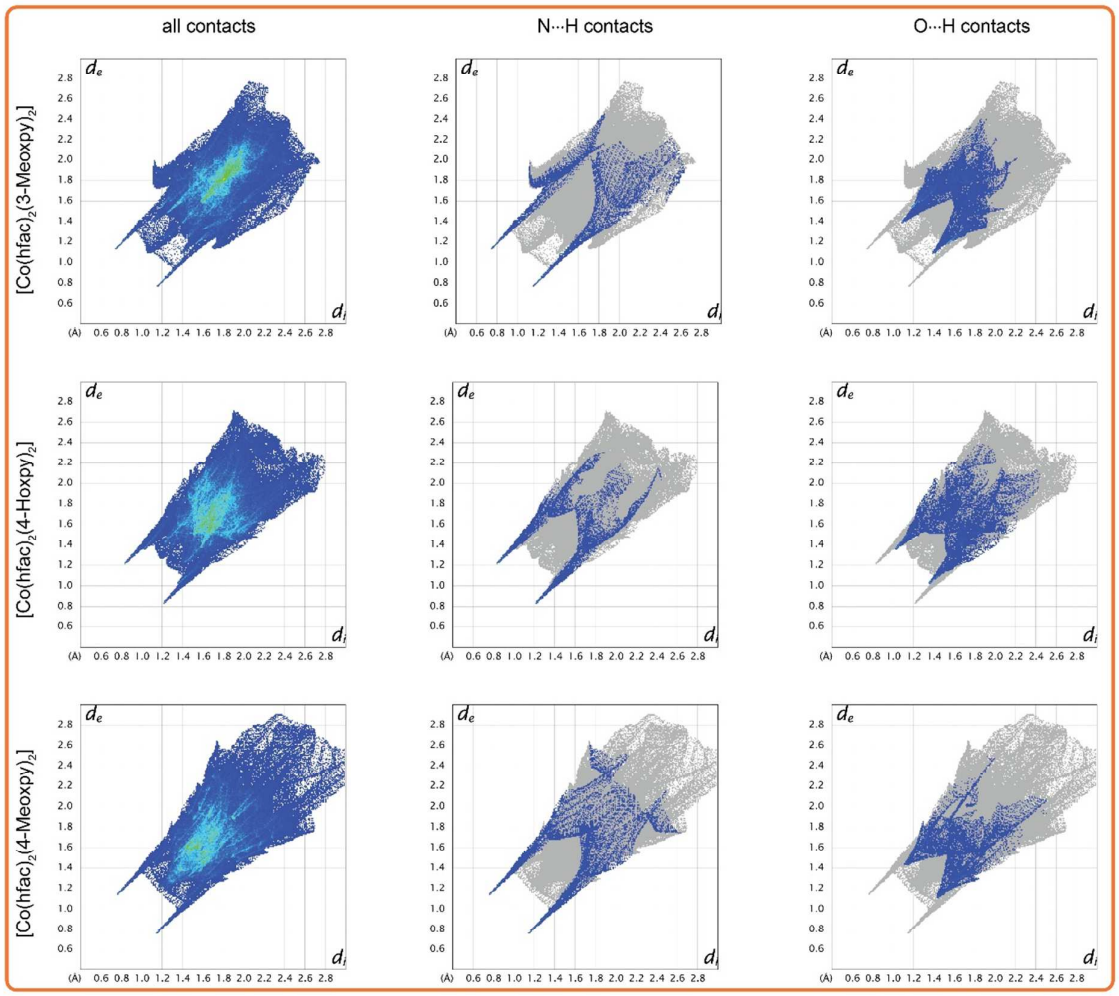

Figure S22. Fingerprint plot for Co(II) complexes with hfac ligand resolved into N···H and O···H contacts. The orange rounded rectangular marks the complexes with O–H···N interaction.